doi.org/10.36721/PJPS.2026.39.7.182.1

Synthesis and biological evaluation of thiophene based oxadiazole derivatives as promising anticancer agents against liver cancer

Zainib Razzaq, Samreen Gul Khan*, Kiran Aftab and Fozia Anjum
Department of Chemistry, Government College University, Faisalabad, Pakistan

Abstract: **Background**: Liver cancer is a leading cause of cancer-related mortality worldwide. Clinical use of the first-line drug sorafenib is limited due to drug resistance and severe adverse effects. **Objectives**: The current study aimed to synthesize a series of *N*-arylated thiophene-based 1,3,4-oxadiazole derivatives containing a carbamothioate moiety (7a-7d) as potential anticancer agents with improved efficacy and safety profiles. **Methods**: Derivatives were synthesized via coupling of thiophene-based 1,3,4-oxadiazole (compound 1) with various electrophiles, yielding 62-86%. The structures of all derivatives were established based on FT-IR, ^{1}H NMR, ^{13}C NMR, and EI-MS. The *in-vitro* anticancer effect of all derivatives was assessed using the MTT assay against the HepG2 cancer cell line and their hemolytic safety was assessed on human red blood cells. **Results**: All derivatives exhibited cytotoxicity with minimal hemolytic effects. Derivative 7b (2,6-dimethyl) exhibited excellent activity by reducing cell viability of 33.96 ± 2.47% at 100 µg/mL and minimal hemolysis (1.20 ± 0.01%) with a high selectivity index (SI) of 28.3, similar to sorafenib (34.32 ± 1.91%, SI = 27.45). Derivatives 7a (phenyl) and 7d (ethyl) showed moderate activity and 7c (fluoro) was the least potent. **Conclusion**: Thiophene-based oxadiazole-coupled carbamothioate derivatives, particularly 7b, demonstrate enhanced anticancer efficacy and safety compared to sorafenib, representing promising candidates for targeted liver cancer therapy.

Keywords: Anticancer activity; Carbamothioate; 5-Chlorothiophene-2-carboxylic acid; 1,3,4-Oxadiazole; Hemolytic activity

Submitted on 14-04-2025 – Revised on 11-09-2025 – Accepted on 11-10-2025

INTRODUCTION

Cancer remains a significant global health concern due to its association with different diseases that impact various organs throughout the body (Hawash *et al.*, 2024). Currently it ranks as the world's second most prevalent cause of death (Feng *et al.*, 2024; Sonal *et al.*, 2024; Sung *et al.*, 2021). This process typically starts whenever a cell grows and replicates abnormally, exceeding normal limits (Mughees *et al.*, 2022). By 2030, cancer is expected to affect approximately twenty-six million new individuals annually, resulting in nearly seventeen million deaths each year (Tayanloo-Beik *et al.*, 2024). Liver cancer is regarded to be one of the most prevalent forms of cancer in the gastrointestinal tract (Suresh *et al.*, 2020). At present, sorafenib is the sole FDA-approved drug for liver cancer treatment, providing only a limited extension of patient survival by a few months (Liang, 2024). However, standard clinical treatments, such as immunotherapy, hormone therapy, radiotherapy, chemotherapy and surgery, often result in significant adverse effects. Furthermore, liver cancer cells exhibit an innate resistance to conventional chemotherapy and radiotherapy (Zhou *et al.*, 2024). To meet the urgent need for discovering and developing effective chemotherapeutic agents and to overcome the challenges of existing anticancer drugs, including toxicity and the development of drug resistance, researchers are actively working on the discovery of effective heterocyclic motifs (Bin Muhsinah *et al.*, 2024).

Several studies explored the applications of distinct nitrogen- and sulfur-containing heterocycles, especially thiophene and 1,3,4-oxadiazole, in drug discovery due to their broad pharmacological potential (Sharma *et al.*, 2024; Thakur *et al.*, 2025). Compounds with a thiophene core demonstrate strong anti-cancer properties by influencing various critical pathways involved in cancer (Almatari *et al.*, 2024). Whereas the 1,3,4-oxadiazole moiety was initially recognized as a key structural component in many therapeutically promising anti-cancer drugs due to its ability to improve metabolic stability and target interaction (Samanta *et al.*, 2025). Carboxamides serve as valuable pharmacophores in numerous pharmacologically active compounds (Al-Najdawi *et al.*, 2025; Javed *et al.*, 2023; Naseer *et al.*, 2022). A number of carboxamide-containing heterocyclic compounds have been found to be useful medications for the treatment of cancer (Mara *et al.*, 2025). Considering the anticancer properties of thiophene, 1,3,4-oxadiazole and carboxamide moieties, we designed and synthesized hybrid compounds incorporating a carbamothioate fragment with two significant bioactive heterocyclic moieties, thiophene and 1,3,4-oxadiazole, aiming to inhibit tumor progression and enhance anticancer efficacy against liver carcinoma (HepG2). Moreover, our molecular design incorporates a hydrophobic aryl ring flanking the carboxamide moiety, thereby enhancing solubility, bioavailability and drug-like properties. In our previous work, we successfully synthesized hybrid compounds incorporating both oxadiazole and carbamothioate pharmacophores to inhibit the progression of epilepsy (Rasool *et al.*, 2023). Continuing from our prior research on heterocyclic compounds, we have now formed a five-membered heterocycle, specifically a 5-(5-chlorothiophen-2-yl)-1,3,4-oxadiazole-2-thiol nucleus, to further explore its potential as a therapeutic agent by

**Corresponding author:* e-mail: samreengul@gcfu.edu.pk

cyclizing the -COOH group of 5-chlorothiophene-2-carboxylic acid.

MATERIALS AND METHODS

General

The chemicals utilized in the present research were of synthetic grade and obtained from Merck and Sigma-Aldrich. Melting points of all derivatives were measured using a Stuart-digital melting point apparatus (SMP 20, UK). Fourier Transform Infrared (FT-IR) Spectroscopy (4000-400 cm^{-1}) was performed using a Shimadzu FT-IR-8400 spectrophotometer (Shimadzu, Japan). A Bruker Avance spectrometer (Bruker, Germany) was used to record proton nuclear magnetic resonance (^{1}H NMR) and carbon-13 nuclear magnetic resonance (^{13}C NMR) spectra at 400 and 101 MHz, respectively, using DMSO-d_6 in tubes of 5 mm diameter. In relation to the internal standard tetramethylsilane (TMS), chemical shift measurements were expressed in the ppm scale and coupling constant values in Hz. Reaction progress and purity of synthesized derivatives were monitored using thin-layer chromatography (TLC) on silica-coated plates (Merk, Germany) using various proportions of n-hexane-ethyl acetate as a solvent system.

Synthesis of methyl 5-chlorothiophene-2-carboxylate (2)

In a 500 mL round-bottom (RB) flask pre-dried in an oven, 5-chlorothiophene 2-carboxylic acid (1; 0.03 mol, 6.0 g) in 30-50 mL of methanol along with a catalytic amount of concentrated Sulphuric acid (2-5 mL) was refluxed at 200 °C for 6-8 hours. The reaction progress was observed using thin-layer chromatography (TLC). Upon completion, the reaction mixture was neutralized with 10% Na_2CO_3 solution. Then, the reaction mixture was shifted to a 1000 mL separating funnel with chloroform ($CHCl_3$) in it. The contents were vigorously shaken for 35-40 minutes, allowing the formation of two distinct layers. After this, the chloroform layer was evaporated to isolate the desired compound (2), which appeared as a brownish oily liquid (Gul *et al*., 2017).

Synthesis of 5-chlorothiophene-2-carbohydrazide (3)

A solution of methyl 5-chlorothiophene-2-carboxylate (2; 0.02 mol, 5.0 mL) in 15 mL methanol was combined with hydrazine monohydrate (0.04 mol, 10 mL) in a 250 mL round-bottom (RB) flask. The reaction mixture was continuously stirred at RT for 1-2 hours at 200 rpm. The reaction progress was observed using thin-layer chromatography (TLC). Upon completion, the resulting precipitate (3) was quenched with cold distilled water, then collected by filtration, washed and dried. Re-crystallization was carried out using methanol (CH_3OH). The desired compound is isolated as a white amorphous solid (Alderawy *et al*., 2020).

Synthesis of 5-(5-chlorothiophen-2-yl)-1,3,4-oxadiazole-2-thiol (4)

In a round-bottom (RB) flask, pre-dried in an oven, a solution of 5-chlorothiophene-2-carbohydrazide (**3**; 0.028 mol, 5 g) in 40 mL absolute methanol was reacted with KOH (0.027 mol, 1.57 g) at reflux for 1 hour. Carbon disulfide (0.027 mol, 1.70 mL) was subsequently added and the mixture was refluxed at 250 °C for 12 to 14 hours. Using thin-layer chromatography (TLC), the reaction's progress and completion were continuously monitored. Upon completion of the reaction, the mixture was diluted using chilled water and diluted HCl was used to reduce the pH below 5-6. The resulting precipitates were separated upon filtration and then subsequently washed with water. Precipitates underwent recrystallization using ethanol. Compound (4) was isolated as a white powder (Khan *et al*., 2020).

Synthesis of N-substituted Aryl & Alkyl 2-bromopropanamides (6a-6d)

In a round-bottom (RB) flask, pre-dried in an oven, aryl & alkyl amines (5a-5d: 0.012 mol) were solubilized in 10.0 mL of 5% Na_2CO_3 solution (pH: 8-9). The previously described reaction mixture was gradually supplemented with 2-bromopropanoyl bromide (0.012 mol). Precipitates were formed by slowly shaking the mixture in the RB flask for 10-15 minutes. Using thin-layer chromatography (TLC), the reaction's progress and completion were continuously monitored. After the reaction was complete, the flask was filled with cold water. The precipitates of electrophiles (6a-6d) were collected by filtration, then dried or recrystallized from methanol (Irfan *et al*., 2024).

Synthesis of N-arylated 5-(5-chlorothiophen-2-yl)-1,3,4-oxadiazole-2-yl-2 sulfanyl carbamide derivatives (7a-7d)

A series of derivatives (7a-7d) was prepared with a favorable yield via reacting compound (4) (0.0004573 mol, 0.1 g) with an equimolar quantity of *N*-substituted aryl & alkyl 2-bromopropanamides (6a-6d) in 6 mL N,N-dimethylformamide (DMF) and LiH (0.002 mol, 0.05 g) through stirring at room temperature (RT) for 3-5 hours. Using thin-layer chromatography (TLC), the progress and completion of the reaction were continuously monitored. Upon completion of the reaction, n-hexane was added, causing precipitation of the desired derivatives (7a-7d). Following recrystallization in methanol or column separation using a combination of ethyl acetate or petroleum ether (2:8), these precipitates were purified (Rasool *et al.*, 2023).

Biological screening

In-vitro cytotoxicity assay

The synthesized thiophene-oxadiazoles (7a-7d) were evaluated *in-vitro* for their anti-hepatocellular activity against the HepG2 liver cancer cell line using the standard 3-(4,5-dimethylthiazol-2-yl)-2,5-diphenyltetrazolium bromide (MTT) assay (Mahmood *et al*., 2022; Akhter *et al*., 2023). The details of cell line source and authentication is provided in supplementary data. The hepatic cancer cells

were cultivated in Dulbecco Modified Eagle Medium (DMEM) added with 10% fetal bovine serum (FBS), 100 units/mL penicillin and 1% streptomycin and incubated at 37 °C in a humidified environment containing 95% air and 5% CO_2. The HepG2 cancer cell line was subjected to treat with the derivatives 7a-7d (100 µg/100 mL) dissolved in dimethyl sulfoxide (DMSO), whereas the cells treated with dimethyl sulfoxide (DMSO) served as a negative control. Cancerous cells were cultivated in 96-well plates and incubated overnight, then subjected to different concentrations of derivatives (7a-7d) 48 h later. After 48 h of incubation, 10 µL of MTT reagent (5 mg/mL) was added to each well and the plates were subsequently incubated for 4 h at 37 °C. After that, 150 µL of control dimethyl sulfoxide (DMSO) was used to dissolve the formazan crystals. A microplate reader was used to measure absorbance at 490 nm in order to determine the percentage of cell viability.

Hemolytic assay

The hemolytic activity of synthesized derivatives (7a-7d) was measured according to the previously reported procedure with small modifications (Gul *et al*., 2017). To isolate red blood cells (RBCs), a fresh blood (3-5 mL) sample was obtained from a healthy donor in an EDTA tube and centrifuged at 1000 rpm (or 1000×g) of the centrifugal force for 5-10 minutes. The tubes were centrifuged, the supernatant discarded and the red blood cell (RBC) pellets cleaned with chilled sterile phosphate-buffered saline (PBS, pH 7.4) three times. After 30 to 60 minutes, 20 µL of the test sample solution (10 mg/mL) made in dimethyl sulfoxide (DMSO) was added to RBC suspension and the mixture was incubated at 37 °C. After that the tubes were placed on ice and recentrifuged for five minutes at 100×g or 13,000 rpm. The supernatant of each tube was shifted into a fresh tube, vortexed with cold PBS and the absorbance was measured at 576 nm. In every experiment, 2,2-azino-bis (3-ethylbenzothiazoline-6-sulfonic acid) ABTS was employed as the positive control and dimethyl sulfoxide (DMSO) as the negative control. The percentage of hemolysis was computed by the following formula:

$$\% \text{ Age Hemolysis } = \frac{(\text{Absorbance of Sample} - \text{Absorbance of Negative Control})}{(\text{Absorbance of Positive Control})} \times 100$$

Statistical analysis

All calculations were carried out in triplicate and statistical analysis was conducted using Microsoft Excel 2013. Results are expressed as: Mean ± S.D (n=3).

RESULTS

The aim of this study was to synthesize derivatives derived from 5-(5-chlorothiophen-2-yl)-1,3,4-oxadiazole-2-yl-2-sulfanyl carbamide and to evaluate their *in-vitro* anticancer activity against the liver cancer HepG2 cell line and hemolytic activity using human red blood cells (RBCs) in order to determine the safety and selectivity of these derivatives. A series of four derivatives was synthesized as shown in Fig. 1.

Chemistry

In summary, 5-chlorothiophene-2-carboxylic acid (1) was subjected to esterification with absolute methanol using conc. H_2SO_4 as a catalyst at 200 °C for 6-8 hours to obtain the corresponding ester (with 90% yield) (2). The ester was gradually stirred with hydrazine monohydrate in methanol (CH_3OH) at 200 rpm for 1-2 hours, resulting in the formation of the respective hydrazide (3) in 80% yield. The hydrazide (3) was then converted into the corresponding oxadiazole (with 75% yield) (4) by progressively heating it with CS_2 in absolute methanol in basic media for 12-14 hours at 250 °C. Various *N*-substituted aryl & alkyl 2-bromopropanamides (6a-6d) were synthesized via reacting different aryl & alkyl amines (5a-5d) with 2-bromopropanoyl bromide in Na_2CO_3 solution (pH: 8-9), serving as electrophiles. These electrophiles (6a-6d) were coupled with compound (4) by substituting the acidic proton of the thiol group at room temperature in N,N-dimethylformamide (DMF) using lithium hydride (LiH) as a catalyst to attain the desired derivatives (7a-7d) in 62-86% yield. The general synthetic route and molecular structures of these derivatives (7a-7d) are shown in Fig. 1.

In-vitro anticancer activity

The *in-vitro* anticancer activity of all the synthesized thiophene-oxadiazole derivatives (7a-7d) was assessed against liver cancer cell line HepG2 at a fixed concentration of 100 µg/mL using the standard MTT protocol to measure cell viability relative to reference standard drug Sorafenib (10 µM), as depicted in Table 1. All derivatives exhibited different cytotoxic effects. In comparison to other derivatives, the thiophene oxadiazole hybrid 7b with a 2,6-dimethyl substituent exhibited the strongest and most significant cytotoxicity, reducing the viability of HepG2 to 33.96 ± 2.47% and being statistically more potent ($p < 0.01$) than Sorafenib. Derivative 7d (4-ethyl) demonstrated promising inhibition with a cell viability of 37.21 ± 1.71%, equivalent to Sorafenib. Comparatively, 7a (phenyl) demonstrated moderate inhibition (52.64 ± 0.25%), whereas 7c (4-fluoro) was found to be the least active (63.98 ± 1.67%) and its effect was not statistically significant compared to sorafenib. These results indicate that the presence of electron-donating groups (dimethyl and ethyl) is preferable toward anticancer activity, whereas electron-withdrawing fluorine inhibits cytotoxic potential.

Hemolytic potential

The hemolytic potential of all thiophene-oxadiazole derivatives (7a-7d) was measured by using human erythrocytes (of a healthy donor) and the results are tabulated in Table 1. All test derivatives exhibited a low to moderate toxicity to red blood cells (RBCs) in comparison to positive control ABTS (95.5%). The most hemocompatible derivative was 7b (2,6-dimethyl) with 1.20 ± 0.01% hemolysis, followed by Sorafenib (1.25 ± 0.02%) and 7a (4.21 ± 0.01%). Derivative 7d presented moderate toxicity (4.35 ± 0.21%), whereas 7c (4-fluoro)

showed the highest toxicity among all derivatives (7.37 ± 0.38%), perhaps indicating a less safe profile. The negative control DMSO (0.1%) and buffer control phosphate-buffered saline (PBS) (0.45 ± 0.15%) verified the assay performance.

Selectivity index

To determine the therapeutic safety of thiophene oxadiazole hybrids (7a-7d), the selectivity index (SI) was calculated by the ratio of cell viability to hemolysis, as shown in Table 1. The selectivity index (SI) value of derivative 7b was the best (28.30), even better than that of Sorafenib (27.45), indicating the excellent balance between cytotoxicity and hemocompatibility. Compound 7a displayed a relatively high selectivity index (12.50), compared with 7c (8.68) and 7d (8.55). These results confirm that dimethyl substitution improves anticancer activity and safety, so 7b is regarded as the most promising lead structure among all synthesized derivatives.

Does response analysis

All prepared derivatives (7a-7d) were further screened individually in dose-response assays (3.1-200 µg/mL) to analyze their concentration-dependent cytotoxic effect on HepG2 cells as shown in Fig. 2. The graphs demonstrated that even at reduced concentrations (25 µg/mL), the derivative 7b (2,6-dimethyl) exhibited positive results, as it reduced the cell viability below 50, indicating its high potency. For the derivative 7d (4-ethyl), slightly higher concentrations were needed to make a significant reduction in viability compared to 7b. Derivatives 7a (phenyl) and 7c (4-fluoro) are the weakest regarding their dose responses, with observable cytotoxicity at higher doses only (100 µg/mL or more). These results validate that the anticancer effect is enhanced with electron donating (dimethyl and ethyl) at lower doses but reduced at higher doses with electron withdrawing (fluoro). Both fixed-dose screening and detailed dose-response analysis identify derivative 7b as the most promising lead candidate overall.

DISCUSSION

The morphology and structures of all produced derivatives (7a-7d) were thoroughly corroborated through detailed spectroscopic analysis. The spectroscopic data confirm the structures of the synthesized derivatives as presented in Table 2. The structural analysis of one representative derivative is presented here for the readers' understanding. Derivative 7b was obtained as a white amorphous powder with a melting point of 141-143°C. Elemental analysis (CHN) data verified its molecular formula, $C_{15}H_{12}ClN_3O_2S_2$, while its molecular weight was validated through the peak of the molecular ion at *m/z* 367.00 $[M+H]^+$. Additionally, structural identification was further confirmed by the proton count and the carbon resonances identified in the ^1H NMR and ^{13}C NMR spectrums, respectively. The FT-IR spectrum (KBr, cm^{-1}), indicated the presence of key functional groups (N-H, Ar. C-H, C=O, C=N, C=C, CH_3 rocking, C-O-C, C-C, C-S-C bending, C-Cl, C-H bending) with absorption bands at υ 3285, 2975, 1635, 1575, 1536, 1375, 1029, 1005, 969, 657, 537 and 504. In the ^{1}HNMR spectrum of derivative 7b, the carboxamide fragment was confirmed by a highly deshielded singlet of N-H in the aromatic region at δ 11.03 ppm. The thiophene ring system attached to the nitrogen atom of the 1,3,4-oxadiazole core was confirmed by two doublets at δ 7.58 ppm and 7.31 ppm (Ar-H-3, H-4) with a coupling constant of 4.0 Hz. A dimethyl-substituted phenyl ring linked with the nitrogen atom of the carboxamide fragment was identified by a doublet of two protons (Ar-H-3′, H-5′) at 7.19 ppm with a coupling constant of 8.3 Hz and a doublet of doublets for one proton (Ar-H-4′) at 7.03 ppm with a coupling constant of 4.5 Hz. In the aliphatic region, a characteristic multiplet for six protons ($2CH_3$) at δ 2.16-2.07 was indicative of two methyl substituents at the phenyl amide ring. The ^{13}CNMR spectrum of derivative 7b displayed signals for ten distinct carbon atoms, accounting for a total of fourteen carbon atoms in the molecule. The carboxamide fragment was verified by downfield resonance of the C=O group at δ 160.84 ppm. The thiophene ring system was identified by two quaternary carbon signals at δ 133.70 ppm and 128.80 ppm (C2, C5) and two methine carbon signals at δ 126.22 ppm and 128.99 ppm (C3, C4). Similarly, a quaternary carbon signal at δ 157.29 ppm (C7) verified the presence of the (1,3,4-oxadiazole-2yl) sulfanyl moiety. The dimethyl-substituted phenyl ring was characterized via three quaternary carbon resonances at δ 136.56 (C1′) and 129.97 ppm (C2′, C6′), along with one symmetrical aromatic methine doublet at δ 129.64 (C3′, C5′) and an aromatic methine signal at δ 126.22 (C4′). A resonance at δ 17.46 ppm confirmed the presence of dimethyl substituents at the phenyl amide ring. The chemical shift values in the ^{1}H NMR (A) and ^{13}C NMR (B) spectrums of derivative 7b are presented in Fig. 3. Based on spectral data, the molecular structure was identified as S-(5-chlorothiophen-2-yl)-1,3,4-oxadiazol-2-yl (2,6-dimethylphenyl)-carbamothioate (7b). The same spectroscopic strategy was employed for structural characterization of the remaining derivatives (7a-7d) in the series.

Biological activity

The synthesized thiophene-oxadiazole derivatives (7a-7d) were evaluated to determine their anticancer activity against HepG2 liver cancer cells and hemolytic activity to evaluate biocompatibility. The results showed distinct structure-activity relationships that depended on the type of substituents on the phenyl ring that was connected to the carboxamide moiety's nitrogen. Among all tested derivatives, derivative 7b (2,6-dimethyl) exhibited excellent activity, with cell viability of 33.96 ± 2.47% at 100 µg/mL. Derivative 7b demonstrated significantly lower hemolysis (1.20 ± 0.01%) than sorafenib (1.25 ± 0.21%) and its efficacy was nearly identical to that of the reference drug sorafenib (34.32 ± 1.91%).

Table 1: Evaluation of anticancer activity against the HepG2 cell line (cell viability % ± SD at 100 µg/mL for test compounds and 10 µM for sorafenib as a reference drug), hemolytic activity (% ± SD) on human RBCs [ABTS (*+ve* control), DMSO (*+ve* control), PBS (buffer control)] and Selectivity Index (viability/hemolysis) of synthesized thiophene-based oxadiazole derivatives (7a-7d).

Compound	Substituents (R)	Cell viability (%)	Hemolytic potential (%)	Selectivity index (SI)	Significance Vs Sorafenib
7a	Phenyl	52.64 ± 0.25	4.21 ± 0.01	12.50	*
7b	2,6-Dimethyl	33.96 ± 2.47	1.20 ± 0.01	28.3	**
7c	4-Fluoro	63.98 ± 1.67	7.37 ± 0.38	8.68	NS (Non-Significant)
7d	4-Ethyl	37.21 ± 1.71	4.35 ± 0.21	8.55	*
Sorafenib (10 µM)		34.32 ± 1.91	1.25 ± 0.21	27.45	Reference
ABTS	*+ve* Control	-	95.5 ± 0.0	-	-
DMSO	*-ve* Control	100 ± 0	0.1	-	-
PBS	Buffer Control	-	0.45 ± 0.15	-	-

The mean ± SD (n=3) is used to express the values. All calculations were performed in triplicate by using Microsoft Excel 2013. One-way ANOVA with T-test was used to determine statistical significance when compared to PBS control (*p < 0.05, **p < 0.01, **p < 0.001). A greater Selectivity Index (SI) denotes a safer and more selective anticancer activity. SI was calculated as the ratio of % Cell Viability to % Hemolysis.

Table 2: Spectral data for derivatives (7a-7d)

Compounds	Appearance	%Yield	M.P. (°C)	FT-IR (cm^{-1})/^{1}H &^{13}C-NMR (400 MHz & 101 MHz DMSO-d_6)/ EI-MS (*m/z*)
7a	Off-white crystalline	70	132-134	3139 (N-H), 2930 (Ar. C-H), 1650 (C=O), 1494 (C=N), 1414 (Ar. C=C), 1252 (C-O-C), 689 (C-S-C bending), 630 (C-Cl)/ 10.75 (s, 1H, N-H), 7.59 (d, *J* = 7.8 Hz, 2H, Ar-H-2′, H-6′), 7.50 (d, *J* = 4.0 Hz, 1H, Ar-H-3), 7.36 (t, *J* = 8.0 Hz, 2H, Ar-H-3′, H-5′), 7.31 (d, *J* = 4.0 Hz, 1H, Ar-H-4), 7.02 (t, *J* = 7.3 Hz, 1H, Ar-H-4′)/ 159.93, 153.50, 138.84, 132.09, 129.58, 128.96, 128.47, 124.36, 122.52, 117.59/338.97 $[M+1]^+$
7b	White amorphous	86	141-143	3285 (N-H), 2975 (Ar. C-H), 1635 (C=O), 1575 (C=N), 1536 (Ar. C=C), 1375 (CH_3 rocking), 1029 (C-O-C), 1005 (C-C bending), 696 (C-S-C bending), 657 (C-Cl), 537,504 (C-H bending)/ 11.03 (s, 1H, N-H), 7.58 (d, *J* = 4.0 Hz, 1H, Ar-H-3), 7.31 (d, *J* = 4.0 Hz, 1H, Ar-H-4), 7.19 (d, *J* = 8.3 Hz, 2H, Ar-H-3′, H-5′), 7.03 (dd, *J* = 4.5 Hz, 1H, Ar-H-4′), 2.16-2.07 (m, 6H, $2CH_3$)/ 160.84, 157.29, 136.56, 133.70, 129.97, 129.64, 128.99, 128.80, 126.22, 17.46/367.00 $[M+1]^+$
7c	White crystalline	73	239-241	3397 (N-H), 3095 (Ar. C-H), 1628 (C=O), 1572 (C=N), 1533 (Ar. C=C), 1214 (C-F), 1024 (C-O-C), 694 (C-S-C bending), 655 (C-Cl)/ 10.79 (s, 1H, N-H), 7.63 – 7.57 (m, 2H, Ar-H-2′, H-6′), 7.50 (d, *J* = 4.0 Hz, 1H, Ar-H-3), 7.30 (d, *J* = 4.0 Hz, 1H, Ar-H-4), 7.21 (d, *J* = 8.9 Hz, 2H, Ar-H-3′, H-5′)/ 159.93, 159.06, 156.69, 153.52, 135.31, 132.12, 128.96, 128.51, 124.31, 119.25, 119.17, 116.31, 116.08/356.96 $[M+1]^+$
7d	Off-white amorphous	62	190-192	3236 (N-H), 2959 (Ar. C-H), 1625 (C=O), 1575 (C=N), 1512 (Ar. C=C), 1424, 1319 (CH_2, CH_3 bending), 1025 (C-O-C), 698 (C-S-C bending), 618 (C-Cl), 527 (C-H bending)/ 10.46 (s, 1H, N-H), 7.52 – 7.46 (m, 3H, Ar-H-3, H-2′, H-6′), 7.30 (d, *J* = 4.0 Hz, 1H, Ar-H-4), 7.19 (d, *J* = 8.6 Hz, 2H, Ar-H-3′, H-5′), 2.56 (q, *J* = 7.6 Hz, 2H, CH_2), 1.16 (t, *J* = 7.6 Hz, 3H, CH_3)/ 160.04, 153.38, 137.95, 136.55, 132.00, 128.93, 128.78, 128.36, 124.42, 117.70, 27.96, 16.23/367.00 $[M+1]^+$

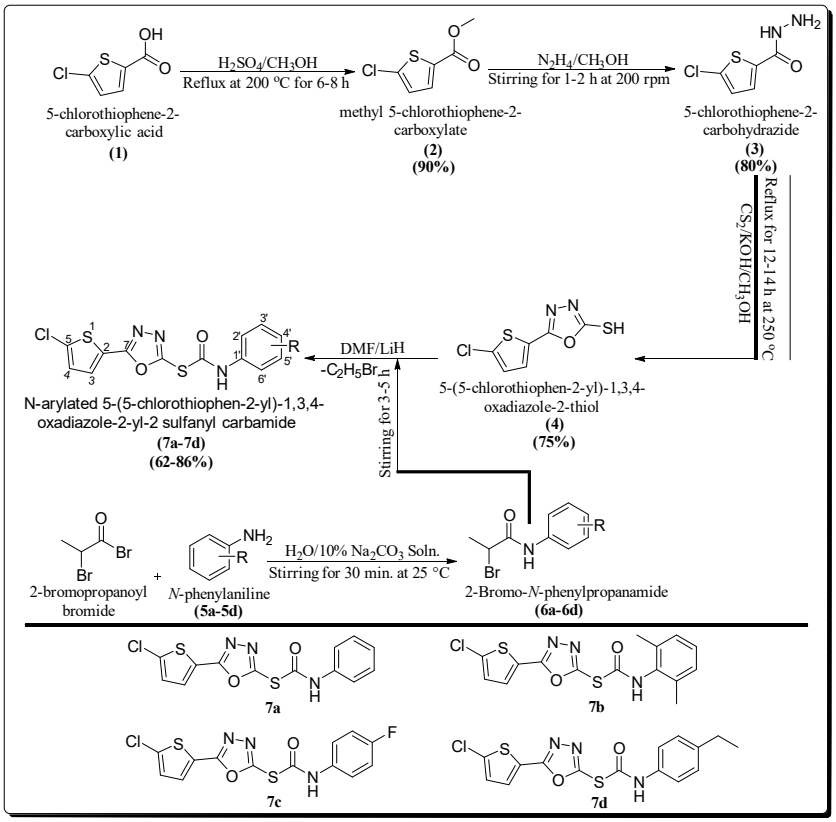

Fig. 1: Outline for synthesis of *N*-arylated 5-(5-chlorothiophen-2-yl)-1,3,4-oxadiazole-2-yl-2 sulfanyl carbamide derivatives (7a-7d).

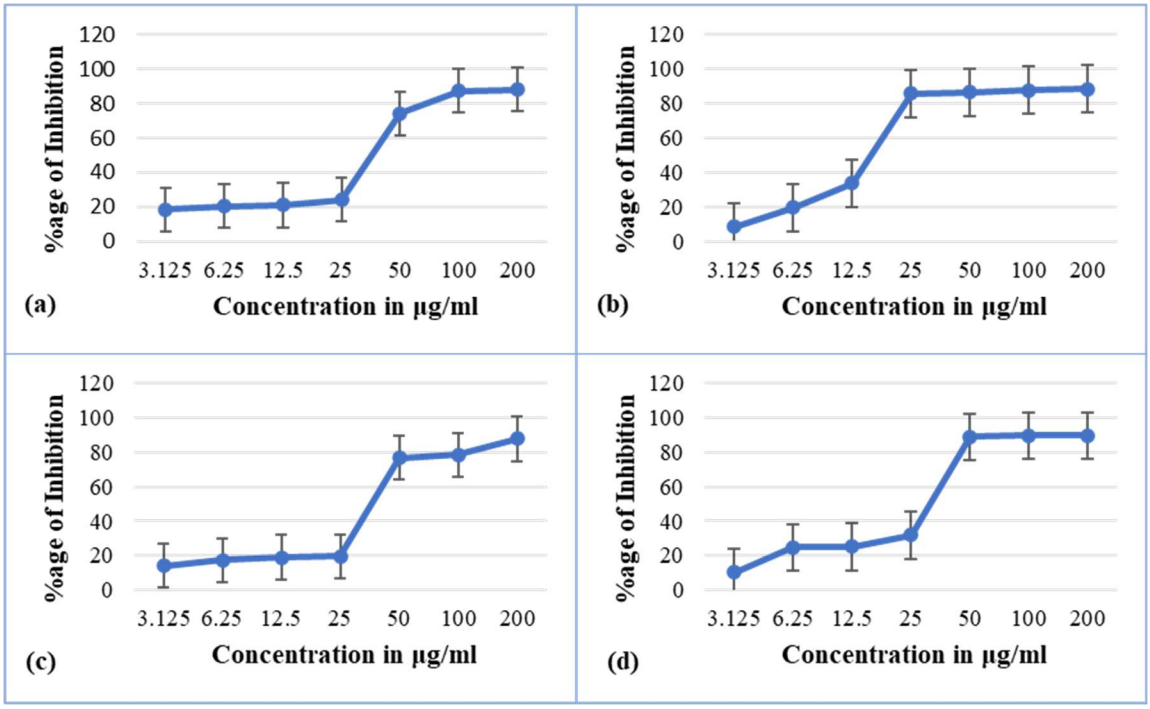

Fig. 2: (a) Dose-response graph for derivative 7a; (b) Dose-response graph for derivative 7b; (c) Dose-response graph for derivative 7c; (d) Dose-response graph for derivative 7d.

doi.org/10.36721/PJPS.2026.39.7.182.1

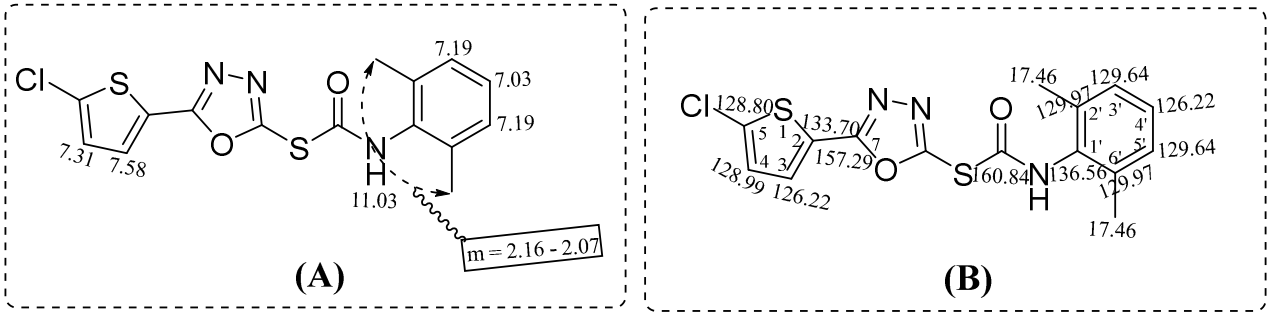

Fig. 3: Chemical Shift values of derivative 7b in (A) ^{1}H-NMR and (B) ^{13}C-NMR.

The selectivity index (SI) of 7b was higher (28.3) than that of sorafenib (27.45), suggesting its superior cytotoxicity against cancer cells compared to red blood cells. It clearly indicates that the presence of steric bulk at *ortho*-positions (2,6-dimethyl) of the phenyl ring increases both potency and safety, as seen in previous reports on methyl-substituted heteroaryl compounds in terms of anticancer research (Benassi *et al.*, 2020; Salem *et al.*, 2022). Derivative 7d (4-ethyl) also showed remarkable cytotoxic activity (37.21 ± 1.71% viability) with a moderate hemolysis (4.35 ± 0.21%) and SI (8.55). While being less selective than 7b, its comparable cytotoxic effect indicates that the small alkyl groups at the phenyl ring also promote an anticancer effect, which is in line with recent research on ethyl-substituted oxadiazole-triazoles (Khedkar *et al.*, 2024). Derivative 7a (phenyl) demonstrated moderate activity with 52.46 ± 0.25% viability and minimal hemolysis (4.21 ± 0.01%) with a resultant SI of 12.5. This suggests that the presence of an unsubstituted bulky phenyl group causes moderate cytotoxicity but reduces selectivity, as instead of 2,6-dimethyl substitution (Bajaj *et al.*, 2021; Romagnoli *et al.*, 2021). Comparatively, the derivative 7c (4-fluoro) substituent at the *para* position of the phenyl ring showed the least activity with 63.98 ± 1.67% viability and higher hemolysis (7.37 ± 0.38%), yielding an SI of 8.68. Previous results suggest that halogenation might preserve polarity without necessarily increasing cytotoxicity. The decreased selectivity of the fluoro substituent revealed the fact that electron-withdrawing substituents at the *para* position of the phenyl ring may disrupt their effectiveness against cancer (Abbas *et al.*, 2024; Wieczorkiewicz *et al.*, 2024). The general pattern of activity was 2,6-dimethyl (7b) ≥ 4-ethyl (7d) ≈ sorafenib ≥ phenyl (7a) ≥ 4-fluoro (7c). Overall, these findings demonstrate that steric and electronic interactions play a crucial role in the regulation of the activity of thiophene-oxadiazole derivatives. Promising candidates for additional preclinical research are electron donating alkyl groups, particularly those with dimethyl functionality, which enhance cytotoxicity and decrease hemolytic toxicity.

CONCLUSION

Thiophene, 1,3,4-oxadiazole and carboxamide scaffolds are important frameworks in anticancer drug discovery. In this study, we synthesized thiophene-based 1,3,4-oxadiazole derivatives (7a-7d), where the carboxamide fragment is linked to a phenyl ring with various substituents and assessed their anticancer effect against HepG2 liver cancer cells as well as hemolytic safety. All derivatives exhibited moderate-to-excellent cytotoxic effects, similar to that of sorafenib, that varied according to the phenyl ring substitution, as indicated in Table 1. The toxicity of these structural hybrids was also low, in the range of 7.37% to 1.20%, as compared to the 95.5% toxicity displayed by the reference standard ABTS. Derivative 7b (2,6-dimethyl) showed excellent anticancer activity, with reduced cell viability of 33.96 ± 2.47% at 100 µg/mL, resulting in a high selectivity index (SI = 28.3), similar to sorafenib. Derivatives 7a (phenyl) and 7d (ethyl) exhibited moderate activity and 7c (fluoro) demonstrated the least activity, with a cell viability of 63.98 ± 1.67%. The general pattern of activity was 2,6-dimethyl (7b) ≥ 4-ethyl (7d) ≈ sorafenib ≥ phenyl (7a) ≥ 4-fluoro (7c). Consequently, these findings suggest that thiophene-oxadiazole-carbamothioate derivatives, especially 7b, have the potential to be a promising lead scaffold for the development of therapeutic candidates against hepatocarcinoma and for overcoming the drawbacks of current therapies such as sorafenib. These findings support further structural optimization and detailed preclinical assessment of these structural hybrids to achieve safe and more effective therapeutic agents for liver cancer.

Acknowledgements

The present work is a part of the PhD thesis research of Zainib Razzaq, conducted under the supervision of Samreen Gul Khan at Government College University Faisalabad, Pakistan. The authors gratefully acknowledge the Department of Chemistry, Government College University Faisalabad, for providing laboratory and

research facilities to carry out the synthesis and biological evaluation studies.

Authors' contributions

Zainib Razzaq: Designed and performed experimental work, data analysis and manuscript writing; Samreen Gul Khan: Supervised the overall research and critically reviewed the manuscript; Kiran Aftab and Fozia Anjum: Contributed to literature review, data interpretation and manuscript editing. All authors read and approved the final version of the manuscript.

Funding

There was no funding.

Data availability statement

All data generated or analyzed during this study are included in this published article. Additional data can be made available from the corresponding author upon reasonable request.

Ethical approval

Hemolytic activity was performed at the Department of Clinical Medicine and Surgery, University of Agriculture, Faisalabad, Pakistan. The study protocol was approved by the institutional ethical committee (approval no. DGS/26077-80, dated 22-07-2023), University of Agriculture, Faisalabad, Pakistan and was conducted in accordance with 1964 Declaration of Helsinki and its subsequent amendments (Hussain *et al.,* 2023).

Conflict of interest

The authors declare no conflict of interest.

Supplementary data

https://www.pjps.pk/uploads/2026/04/SUP1776581182.pdf

REFERENCES

Abbas AA, Farghaly TA and Dawood KM (2024). Recent advances on anticancer and antimicrobial activities of directly-fluorinated five-membered heterocycles and their benzo-fused systems. *RSC Adv.*, **14**(28): 19752-19779.

Al-Najdawi MM, Saleh MM, Sabbah DA, Hajjo R, Zalloum H, Abudoleh SM, Abuarqoub DA, Al-Hiari YM, Mohammad MY, ALSalamat H, Mansour H, Aljbour ND and Mestareehi AH (2025). Exploring carboxamide derivatives as promising anticancer agents: Design, *in-vitro* evaluation and mechanistic insights. *Int. J. Mol. Sci*., **26**(12): 5903.

Almatari AS, Saeed A, Abdel-Ghani GE, Abdullah MMS, Al-Lohedan HA, Abdel-Latif E and El-Demerdash A (2024). Synthesis of some novel thiophene analogues as potential anticancer agents. *Chem. Biodivers*., **21**(7): e202400313.

Alderawy MQA, Alrubaie LAR and Sheri FH (2020). Synthesis, characterization of ibuprofen *N*-acyl-1,3,4-oxadiazole derivatives and anticancer activity against MCF-7 cell line. *Syst. Rev. Pharm.*, **11**(4): 681-689.

Akhter N, Batool S, Khan SG, Rasool N, Anjum F, Rasul A and Imran S (2023). Bio-oriented synthesis and molecular docking studies of 1,2,4-triazole based derivatives as potential anti-cancer agents against HepG2 cell line. *Pharmaceuticals*, **16**(2): 211.

Bajaj S, Kumar MS, Tinwala H and Yc M (2021). Design, synthesis, modelling studies and biological evaluation of 1,3,4-oxadiazole derivatives as potent anticancer agents targeting thymidine phosphorylase enzyme. *Bioorg. Chem*., **111**: 104873.

Benassi A, Doria F and Pirota V (2020). Groundbreaking anticancer activity of highly diversified oxadiazole scaffolds. *Int. J. Mol. Sci*., **21**(22): 8692.

Bin Muhsinah A, Alharbi MM, Kheder NA, Soliman SM, Ghabbour HA, Mahmoud NS, Elhaty IA and Mabkhot YN (2024). New thiophene derivatives: Chemoselective synthesis, antitumor effectiveness, structural characterization, DFT calculations, Hirshfeld surface and Fukui function analysis. *BMC Chem*., **18**(1): 228.

Feng Gh, Yue Qq, Zhao Kh, Peng T, Tang T, Sun Yx, Meng Xr, Huang Ll, Zeng X and Zeng Y (2024). Factors affecting the compliance of hepatocellular carcinoma screening among high-risk populations: A systematic review and meta-analysis. *Public Health Nurs*., **41**(3): 476-486.

Gul S, Abbasi MA, Khan KM, Nafeesa K, Siddiqa A, Akhtar MN and Subhani Z (2017). Synthesis, antimicrobial evaluation and hemolytic activity of 2-[[5-alkyl/aralkyl substituted-1,3,4-oxadiazol-2-yl]thio]-N-[4-(4-morpholinyl)phenyl]acetamide derivatives. *J. Saudi Chem. Soc.*, **21**: S425-S433.

Hawash M, Abdallah S, Abudayyak M, Melhem Y, Abu Shamat M, Aghbar M, Capan I, Abualhasan M, Kumar A, Kaminski M, Goral T, Dominiak PM and Sobuh S (2024). Exploration of isoxazole analogs: Synthesis, COX inhibition, anticancer screening, 3D multicellular tumor spheroids and molecular modeling. *Eur. J. Med. Chem*., **271**: 116397.

Hussain S, Javed W, Tajammal A, Khalid M, Rasool N, Riaz M and Shah SAA (2023). Synergistic antibacterial screening of Cymbopogon citratus and Azadirachta indica: Phytochemical profiling and antioxidant and hemolytic activities. *ACS omega,* **8**(19): 16600-16611.

Irfan M, Khan HA, Bibi S, Wu G, Ali A, Khan, SG, and Chen K (2024). Exploration of nonlinear optical properties of 4-methyl-4*H*-1,2,4-triazol-3-yl) thio)-*N*-phenylpropanamide based derivatives: Experimental and DFT approach. *Sci. Rep*., **14**(1): 2732.

Javed MS, Zubair M, Rizwan K and Jamil M (2023). *In-vitro* anti-microbial activity and anti-cancer potential of novel synthesized carbamothioyl-furan-2-carboxamide derivatives. *Molecules*, **28**(12): 4583.

Khan SG, Bokhari TH, Anjum F, Akhter N, Rasool S, Shah SAA, Shahid M and Arshad A (2020). Synthesis, characterization, antibacterial, hemolytic and thrombolytic activity evaluation of 5-(3-chlorophenyl)-2-((*N*-(substituted)-2-acetamoyl) sulfanyl)-1,3,4-oxadiazole derivatives. *Pak. J. Pharm. Sci*., **33**(1): 871–876.

Khedkar NR, Sindkhedkar M and Joseph A (2024). Computational design, synthesis and assessment of 3-(4-(4-(1,3,4-oxadiazol-2-yl)-1H-imidazol-2-yl)phenyl)-1,2,4-oxadiazole derivatives as effective epidermal growth factor receptor inhibitors: A prospective strategy for anticancer therapy. *RSC Med. Chem*., **15**(5): 1626-1639.

Liang Y (2024). Mechanisms of sorafenib resistance in hepatocellular carcinoma. *Clin. Res. Hepatol. Gastroenterol*., **48**(8): 102434.

Mara BI, Mioc A, Deveseleanu-Corici LN, Soica C and Cseh L (2025). Novel compounds featuring a thiophene carboxamide scaffold: Synthesis, characterization and antiproliferative evaluation. *Int. J. Mol. Sci*., **26**(14): 6823.

Mughees M, Kaushal JB, Sharma G, Wajid S, Batra SK and Siddiqui JA (2022). Chemokines and cytokines: Axis and allies in prostate cancer pathogenesis. *Semin. Cancer Biol*., **86**(Pt 3): 497-512.

Mahmood S, Khan SG, Rasul A, Christensen JB and Abourehab MA (2022). Ultrasound assisted synthesis and in silico modelling of 1,2,4-triazole coupled acetamide derivatives of 2-(4-isobutyl phenyl) propanoic acid as potential anticancer agents. *Molecules*, **27**(22): 7984.

Naseer A, Osra FA, Awan AN, Imran A, Hameed A, Ali Shah SA, Iqbal J and Zakaria ZA (2022). Exploring novel pyridine carboxamide derivatives as urease inhibitors: Synthesis, molecular docking, kinetic studies and ADME profile. *Pharmaceuticals*, **15**(10): 1288.

Rasool N, Razzaq Z, Gul Khan S, Javaid S, Akhtar N, Mahmood S, Christensen JB, Ali Altaf A, Muhammad Muneeb Anjum S, Alqahtani F, AlAsmari AF and Imran I (2023). A facile synthesis of 1,3,4-oxadiazole-based carbamothioate molecules: Antiseizure potential, EEG evaluation and *in-silico* docking studies. *Arabian J. Chem*., **16**(4): 104610.

Romagnoli R, Preti D, Hamel E, Bortolozzi R, Viola G, Brancale A, Ferla S, Morciano G and Pinton P (2021). Concise synthesis and biological evaluation of 2-aryl-3-anilinobenzo[b]thiophene derivatives as potent apoptosis-inducing agents. *Bioorg. Chem*., **112**: 104919.

Salem MM, Ayyad R and Sakr H (2022). Design and synthesis of some new oxadiazole derivatives as anticancer agents. *Int. J. Org. Chem*., **12**(2): 64-74.

Samanta A, Maji A, Paul A, Mishra SS, Nahar S and Maity TK (2025). 1,3,4-Oxadiazole-based EGFR inhibitors as anticancer therapeutics: SAR study and binding mode of interaction analysis. *Eur. J. Med. Chem. Rep*., **14**: 100265.

Sharma U, Kumar R, Mazumder A, Salahuddin, Kukreti N, Mishra R and Chaitanya M (2024). Substrate-based synthetic strategies and biological activities of 1,3,4-oxadiazole: A review. *Chem. Biol. Drug Des*., **103**(6): e14552.

Sonal S, Boudreau C, Lee GC, Cauley CE, Kunitake H, Goldstone RN, Francone TD, Bordeianou LG, Ricciardi R and Berger DL (2024). Causes of death in patients operated for colorectal cancer. *Surgery*, **175**(5): 1285-1290.

Sung H, Ferlay J, Siegel RL, Laversanne M, Soerjomataram I, Jemal A and Bray F (2021). Global cancer statistics 2020: GLOBOCAN estimates of incidence and mortality worldwide for 36 cancers in 185 countries. *CA Cancer J. Clin*., **71**(3): 209-249.

Suresh D, Srinivas AN and Kumar DP (2020). Etiology of hepatocellular carcinoma: Special focus on fatty liver disease. *Front. Oncol*., **10**: 601710.

Tayanloo-Beik A, Eslami A, Sarvari M, Jalaeikhoo H, Rajaeinejad M, Nikandish M, Faridfar A, Rezaei-Tavirani M, Mafi AR, Larijani B and Arjmand B (2024). Extracellular vesicles and cancer stem cells: A deadly duo in tumor progression. *Oncol. Rev*., **18**: 1411736.

Thakur S, Kumar D, Jaiswal S, Goel KK, Rawat P, Srivastava V, Dhiman S, Jadhav HR and Dwivedi AR (2025). Medicinal chemistry-based perspectives on thiophene and its derivatives: Exploring structural insights to discover plausible druggable leads. *RSC Med. Chem*., **16**(2): 481-510.

Wieczorkiewicz PA, Krygowski TM and Szatylowicz H (2024). Substituent effects and electron delocalization in five-membered N-heterocycles. *Phys. Chem. Chem. Phys*., **26**(28): 19398-19410.

Zhou Y, Chen Y, Xuan C, Li X, Tan Y, Yang M, Cao M, Chen C, Huang X and Hu R (2024). DPP9 regulates NQO1 and ROS to promote resistance to chemotherapy in liver cancer cells. *Redox Biol*., **75**: 103292.